

**Biotinylated  
Protein**

Strict quality control

Most Fc receptor

Car-T relevant proteins

Hot Mab drug targets



Sino Biological  
Biological Solution Specialist

High quality  
Next-day shipping

Click



## Dynamics and Transcriptomics of Skin Dendritic Cells and Macrophages in an Imiquimod-Induced, Biphasic Mouse Model of Psoriasis

This information is current as of March 26, 2018.

Dorothea Terhorst, Rabie Chelbi, Christian Wohn, Camille Malosse, Samira Tamoutounour, Audrey Jorquera, Marc Bajenoff, Marc Dalod, Bernard Malissen and Sandrine Henri

*J Immunol* 2015; 195:4953-4961; Prepublished online 14 October 2015;

doi: 10.4049/jimmunol.1500551

<http://www.jimmunol.org/content/195/10/4953>

**Supplementary Material** <http://www.jimmunol.org/content/suppl/2015/10/14/jimmunol.1500551.DCSupplemental>

**References** This article **cites 39 articles**, 13 of which you can access for free at: <http://www.jimmunol.org/content/195/10/4953.full#ref-list-1>

**Why *The JI*? Submit online.**

- **Rapid Reviews! 30 days\*** from submission to initial decision
- **No Triage!** Every submission reviewed by practicing scientists
- **Fast Publication!** 4 weeks from acceptance to publication

*\*average*

**Subscription** Information about subscribing to *The Journal of Immunology* is online at: <http://jimmunol.org/subscription>

**Permissions** Submit copyright permission requests at: <http://www.aai.org/About/Publications/JI/copyright.html>

**Email Alerts** Receive free email-alerts when new articles cite this article. Sign up at: <http://jimmunol.org/alerts>

*The Journal of Immunology* is published twice each month by The American Association of Immunologists, Inc., 1451 Rockville Pike, Suite 650, Rockville, MD 20852  
Copyright © 2015 by The American Association of Immunologists, Inc. All rights reserved.  
Print ISSN: 0022-1767 Online ISSN: 1550-6606.



# Dynamics and Transcriptomics of Skin Dendritic Cells and Macrophages in an Imiquimod-Induced, Biphasic Mouse Model of Psoriasis

Dorothea Terhorst,<sup>\*,†</sup> Rabie Chelbi,<sup>\*,1</sup> Christian Wohn,<sup>\*,1</sup> Camille Malosse,<sup>\*</sup> Samira Tamoutounour,<sup>\*</sup> Audrey Jorquera,<sup>\*</sup> Marc Bajenoff,<sup>\*</sup> Marc Dalod,<sup>\*</sup> Bernard Malissen,<sup>\*,2</sup> and Sandrine Henri<sup>\*,2</sup>

Psoriasis is a chronic inflammatory skin disease of unknown etiology. Previous studies showed that short-term, 5–7 d-long application of imiquimod (IMQ), a TLR7 agonist, to the skin of mice triggers a psoriasis-like inflammation. In the current study, by applying IMQ for 14 consecutive d, we established an improved mouse psoriasis-like model in that it recapitulated many of the clinical and cellular hallmarks observed in human patients during both the early-onset and the late-stable phase of psoriasis. Although macrophages and dendritic cells (DCs) have been proposed to drive the psoriatic cascade, their largely overlapping phenotype hampered studying their respective role. Based on our ability to discriminate Langerhans cells (LCs), conventional DCs, monocytes, monocyte-derived DCs, macrophages, and plasmacytoid DCs in the skin, we addressed their dynamics during both phases of our biphasic psoriasis-like model. Plasmacytoid DCs were not detectable during the whole course of IMQ treatment. During the early phase, neutrophils infiltrated the epidermis, whereas monocytes and monocyte-derived DCs were predominant in the dermis. During the late phase, LCs and macrophage numbers transiently increased in the epidermis and dermis, respectively. LC expansion resulted from local proliferation, a conclusion supported by global transcriptional analysis. Genetic depletion of LCs permitted to evaluate their function during both phases of the biphasic psoriasis-like model and demonstrated that their absence resulted in a late phase that is associated with enhanced neutrophil infiltration. Therefore, our data support an anti-inflammatory role of LCs during the course of psoriasis-like inflammation. *The Journal of Immunology*, 2015, 195: 4953–4961.

Psoriasis is a common inflammatory skin disease characterized by scaly reddish plaques resulting from hyperproliferation and disturbed differentiation of keratinocytes (1). The antimicrobial peptide LL37 produced by keratinocytes has been suggested to contribute to the initiation of the inflammatory psoriatic cascade by forming complexes with extracellular self-nucleic acids present in lesional skin (2). Such complexes have been proposed to reach intracellular compartments of plasmacytoid dendritic cells (pDCs) and conventional DCs (cDCs), where they are recognized by TLR7, -8, and -9 and DNA sensors and cause the production of type I IFN (IFN-I). Activation of dermal cDCs by IFN-I and TLR leads to the production of IL-23 that in turn activates several cell types to make IL-17, resulting in

a neutrophil skin infiltration that characterizes the early phase of psoriasis. Activated dermal cDCs concomitantly migrate to skin-draining lymph nodes (LNs), where they trigger the differentiation of autoantigen-specific naive T cells into skin-tropic effector T cells that are capable of secreting TNF- $\alpha$ , IFN- $\gamma$ , IL-17, or IL-22 and responsible for fueling the late phase of psoriasis (2). These cytokines contribute to increase the numbers of infiltrating neutrophils and stimulate keratinocytes to produce growth factors and inflammatory mediators (3–7).

The skin contains several types of myeloid cells that can be classified by surface markers, anatomical location, and functional properties (8, 9). Langerhans cells (LCs) are the only APC of the epidermis. They derive from precursors that reach the epidermis

<sup>\*</sup>Centre d'Immunologie de Marseille-Luminy, Aix Marseille Université UM2, INSERM, U1104, CNRS UMR7280, 13288 Marseille, France; and <sup>†</sup>Department of Dermatology, Charité University Medicine Berlin, 10117 Berlin, Germany

<sup>1</sup>R.C. and C.W. contributed equally to this work.

<sup>2</sup>B.M. and S.H. contributed equally to this work.

ORCID: 0000-0001-6956-5411 (A.J.); 0000-0002-6436-7966 (M.D.); 0000-0003-1340-9342 (B.M.).

Received for publication March 6, 2015. Accepted for publication September 16, 2015.

This work was supported by CNRS, INSERM, European Communities Framework Program 7 (Novel Drug Delivery Routes Mediated via Nanotechnology Targeting Allergy Vaccination (NANOASIT) Euroanomed Project and Enhanced Epidermal Antigen-Specific Immunotherapy (EE-ASI) European Collaborative Research Project to B.M.), European Research Council Grants (322465 to B.M. and 281225 to M.D.), Agence Nationale de la Recherche (SkinDC to S.H.), the Innate Immunity in Health and Disease (I2HD) Centre d'Immunologie de Marseille-Luminy-Sanofi collaborative project, and by fellowships from Agence Nationale de la Recherche (Nanoasit project; to S.T.) and the Innate Immunity in Health and Disease Centre d'Immunologie de Marseille-Luminy-Sanofi

collaborative project (to D.T., R.C., and C.W.). The France-BioImaging infrastructure supported by Agence Nationale de la Recherche provided support for histological analysis.

The microarray data presented in this article have been submitted to the Gene Expression Omnibus under accession number GSE65309.

Address correspondence and reprint requests to Dr. Bernard Malissen and Dr. Sandrine Henri, Centre d'Immunologie de Marseille-Luminy, Parc Scientifique de Luminy, 13288 Marseille Cedex 9, France. E-mail addresses: bernardm@ciml.univ-mrs.fr (B.M.) and henri@ciml.univ-mrs.fr (S.H.)

The online version of this article contains supplemental material.

Abbreviations used in this article: B6, C57BL/6; BM, bone marrow; cDC, conventional dendritic cell; DC, dendritic cell; DT, diphtheria toxin; GSEA, GeneSet enrichment analysis; IFN-I, type I IFN; IMQ, imiquimod; ISG, IFN-stimulated gene; LC, Langerhans cell; LN, lymph node; MHC II, MHC class II; MMP9, matrix metalloproteinase 9; moDC, monocyte-derived dendritic cell; PCA, principal component analysis; pDC, plasmacytoid dendritic cell; TRITC, tetramethylrhodamine-5-(and-6)-isothiocyanate.

Copyright © 2015 by The American Association of Immunologists, Inc. 0022-1767/15/\$25.00

before birth and self-maintain through local low-level proliferation (10, 11). The dermis contains monocytes, monocyte-derived DCs (moDCs), macrophages, and several subsets of cDCs (8, 12). CD11b<sup>+</sup> dermal cells have been suggested to play a key role in initiating T cell responses in imiquimod (IMQ)-induced psoriasis-like lesions (13, 14). However, those earlier studies overlooked the heterogeneity of CD11b<sup>+</sup> dermal cells and the presence of monocytes, moDCs, macrophages, and DCs among them (8).

Considering that the IMQ-induced mouse model of psoriasis has so far been only used to study the early phase of the disease (15), we adapted it to study both the early and late phases of the disease and better mimic the human condition. By combining this model that relies on long-term IMQ application to our multicolor phenotyping flow cytometry key (8, 9), we succeeded analyzing the dynamics of LCs, cDCs, neutrophils, monocytes, moDCs, pDCs, and macrophages over the course of the inflammation. In contrast to previous transcriptomic studies that involved whole psoriatic skin samples and primarily probed keratinocyte responses (4, 16), we focused our transcriptomic analysis on homogenous populations of LCs, CD11b<sup>+</sup> DCs, monocytes, moDCs, and macrophages sorted from lesional skin at the early and late stages of IMQ-induced psoriasis-like skin inflammation.

## Materials and Methods

### Mice

Mice were housed under specific pathogen-free conditions and used between 6 and 11 wk of age. C57BL/6 (B6) female mice expressing CD45.1 [B6 (CD45.1)] or CD45.2 [B6 (CD45.2)] were purchased from Janvier Laboratories. *LangEGFP* and *LangDTREGFP* (17) mice have been described. All experiments involving mice were done in accordance with French and European guidelines for animal care.

### IMQ-induced psoriatic inflammation

Aldara (MEDA Pharma, Paris, France) is a commercially available cream that contains 5% IMQ. Mice at 6–11 wk of age received on a daily basis and for 14 consecutive d a dose of Aldara cream corresponding to 0.35 mg IMQ per ear side. The severity of inflammation of the ear skin was measured on a daily basis using an adapted version of the clinical Psoriasis Area and Severity Index. Erythema and scaling were scored independently on a scale from 0–4: 0, none; 1, slight; 2, moderate; 3, marked; and 4, very marked. The thickness of both ears was measured using a caliper (Kaefer), and the percentage change from baseline was calculated.

### Immunofluorescence

Ears were fixed in AntigenFix (MMFrance, Francheville, France) for 2 h, then washed in phosphate buffer, and dehydrated in 30% sucrose in PBS. The 30- $\mu$ m frozen sections were stained with Abs. Anti-GFP and anti-phalloidin were from Invitrogen, anti-Ki67 (MIB-5) from DakoCytomation, and anti-matrix metalloproteinase 9 (MMP9; GE-213) from Abcam.

### In vivo LC depletion

*LangDTREGFP* mice were injected i.p. twice and 48 h apart with 1  $\mu$ g diphtheria toxin (DT; Calbiochem, EMD Millipore).

### Isolation of DCs, monocytes, and macrophages from skin and skin-draining LNs

DCs and other myeloid cell types were isolated from lymphoid organs as previously described (12). Briefly, LNs were cut into small pieces and digested for 20 min at room temperature with a mixture of type II collagenase (Worthington Biochemical) and DNase I (Sigma-Aldrich). The resulting cell suspension was treated with 5 mmol EDTA to disrupt DC-T cell conjugates. After eliminating undigested material, light-density cells were enriched by centrifugation on an Optiprep solution ( $d = 1.32$  g/ml; Abcys). To extract skin mononuclear phagocytic cells, ears were split into dorsal and ventral parts and incubated with a solution of PBS containing 1 mg/ml dispase (Roche) for 2 h at 37°C or overnight at 4°C, as specified. The dorsal and ventral parts were then cut into small pieces and incubated for 90 min at 37°C with RPMI 1640 containing 1 mg/ml DNase and 1 mg/ml Collagenase IV (Worthington Biochemical). The resulting single-cell suspension was subjected to centrifugation on a Percoll gradient

(Amersham-Pharmacia) in which cells were resuspended in 70% Percoll and layered under a 40% Percoll layer. The whole skin containing dermis and epidermis was processed except for Fig. 4D, for which epidermis and dermis were analyzed separately.

**Flow cytometry.** Cells were stained and analyzed using an FACS LSRII system using DIVA software (BD Biosciences). Allophycocyanin-Cy7-conjugated anti-NK1.1 (PK136), anti-CD3 (17A2), anti-Ly-6G (1A8), anti-CD19 (6D5), and allophycocyanin- or PE-conjugated anti-CD64 (X54-5/7.1) were from BioLegend. PE-conjugated anti-CCR2 (475301) were from R&D Systems; Alexa 700-conjugated anti-MHC class II (MHC II; I-A/I-E) (M5/114.15.2), PE-Cy5.5-conjugated anti-CD45.2 (104), PE-Cy5.5-conjugated anti-CD45 (30-F11), allophycocyanin-conjugated anti-CD45.1 (A20), and PE-Cy5-conjugated anti-CD24 (M1/69) were all from eBioscience. FITC-conjugated anti-Ly-6C (AL21) was from BD Pharmingen. Biotin-conjugated Abs were detected using streptavidin conjugated with PE-Texas Red (Invitrogen). Prior to analyzing monocytes, macrophages, and DCs, we systematically gated out B cells, T cells, NK cells, and neutrophils using a dump channel corresponding to cells positive for B220, CD3, NK1.1, or Ly-6G cells. Analysis was performed using FlowJo software (Tree Star).

### Skin painting assay

Mice were painted on the back side of the ears with 20  $\mu$ l 0.5% tetramethylrhodamine-5-(and-6)-isothiocyanate (TRITC; Invitrogen) prepared in DMSO and diluted to 0.5% in a 1:1 acetone/dibutylphthalate mixture. The ear of mice treated for 8 d with IMQ were painted with 20  $\mu$ l TRITC solution. IMQ treatment was then continued for 3 more d prior to collecting auricular LNs and analyzing their cellular content by flow cytometry. Untreated mice were painted with TRITC and used as controls.

### BrdU and Ki67 analysis

Mice were treated for 5 or 11 d with IMQ and BrdU was administered continuously for the last 4 d of IMQ treatment. Untreated control mice were subjected to BrdU administration for 4 d. To ensure the immediate availability of BrdU (Sigma-Aldrich), mice were injected i.p. with 1.5 mg BrdU, and their drinking water was supplemented for 4 d with 0.8 mg/ml BrdU and 2% glucose and changed daily. The skin of control mice and IMQ-treated mice was analyzed after 4 d of BrdU administration. DCs from total skin were first stained for surface markers and then fixed and permeabilized for BrdU staining (BrdU labeling Flow kit; BD Biosciences). Staining for Ki-67 (BD Biosciences) was performed using the BrdU labeling Flow kit protocol.

### Generation of bone marrow chimera

The 7- to 8-wk-old B6 (CD45.1  $\times$  CD45.2) mice were lethally irradiated with two doses 5 h apart and then injected i.v. with  $2 \times 10^6$  bone marrow (BM) cells. BM cells were obtained from femurs and tibias of wild-type B6 (CD45.1) mice. Analysis of monocytes, neutrophils, and B cells present in the blood of the chimeras for expression of CD45.1, and lack of CD45.2 expression was used to assess proper BM engraftment.

### Cell sorting

For microarray analyses, skin myeloid cells were sorted according to the marker combination described in Supplemental Table I and Supplemental Fig. 1. The smaller frequency of Ly-6C<sup>low</sup> moDCs and CD11b<sup>-</sup>CD24<sup>+</sup> and CD11b<sup>-</sup>CD24<sup>-</sup> DCs found in IMQ-treated skin prevented their analysis.

### RNA isolation and microarray analyses

Qiagen micro RNAeasy PLUS kit (Qiagen) was used to extract total RNA from FACS-sorted cells. Quantity, quality, and absence of genomic DNA contamination were assessed with a Bioanalyser (Agilent Technologies). Biotinylated double-strand cDNA targets were prepared, starting from 4.9 to 20 ng total RNA using the NuGEN Ovation Pico WTA System V2 Kit and the NuGEN Encore Biotin Module Kit according to NuGEN recommendations. Following fragmentation and end labeling, 2  $\mu$ g cDNAs was hybridized for 16 h at 45°C on GeneChip Mouse Gene 1.0 ST arrays (Affymetrix) interrogating 28,853 genes represented by  $\sim 27$  probes spread across the full length of the gene. The chips were washed and stained in the GeneChip Fluidics Station 450 (Affymetrix) and scanned with the GeneChip Scanner 3000 7G (Affymetrix) at a resolution of 0.7  $\mu$ m. Microarray analyses were performed as previously described (18–20). Hierarchical clustering and principal component analysis (PCA) were performed on the 5558 probes showing a fold change  $\geq 2$  and a  $p$  value  $< 0.05$  for at least one cell type between day 5 or 11 versus day 0 using the LIMMA statistical package of the R program. The distance metric/linkage parameters used for hierarchical clustering were Pearson and average. The robustness of nodes was calculated as the percentage of occurrence of this node

among 1000 independent trees generated by multiscale bootstrap resampling. The nodes of the hierarchical clustering analysis for which values are not indicated correspond to 100% (Fig. 3A). Quality controls assessing the technical accuracy of data generation, the close proximity of most biological triplicates in hierarchical clustering, and the recovery of the expected cell type-specific transcriptomic fingerprints in steady state and IMQ-treated conditions confirmed the accuracy and robustness of the gene expression profiles that were obtained (Fig. 3A and data not shown).

#### Statistical analyses

For data other than microarray analyses, the unpaired Student *t* test was used for statistical analyses with GraphPad Prism software (GraphPad) (\**p* < 0.05, \*\**p* < 0.01, \*\*\**p* < 0.005).

#### Accession numbers

The microarray data are available in the Gene Expression Omnibus database (<http://www.ncbi.nlm.nih.gov/gds>) under the accession number GSE65309.

## Results

### Long-term application of IMQ on mouse skin recapitulates the early and late phases of human psoriasis

Topical treatment of mouse skin with Aldara cream containing IMQ triggers a psoriasis-like inflammation (21). In most models, 6.25 mg Aldara cream is applied on recently shaved back skin. Depilation induces LC activation (17), so we selected the ear to apply Aldara cream because it has only sparse hair follicles that preclude prior depilation. By using 7 mg Aldara cream (0.35 mg IMQ) per ear side, we induced the full flare of psoriatic skin inflammation. In contrast to most previous conditions in which treatment was limited to 5–7 d, we applied Aldara cream for 14 consecutive d. As documented below, this regimen allowed the study of the early acute phase and late chronic phase of the resulting psoriasis-like inflammation. Using an adapted human psoriasis activity and severity score, clinical parameters such as skin thickness, erythema, and scaling continuously increased over the first 7 d of application, denoted as the early phase, and reached a plateau by day 7. During the late phase (days 8–14), those clinical parameters remained stable (Fig. 1A).

Histopathological examination of the psoriasis-like lesions that developed over the course of IMQ treatment further supported the existence of distinguishable early and late phases (Fig. 1B). The first changes appearing during the early phase corresponded to dense dermal infiltrate and dilatation of blood vessels. The plaques that developed during the early phase were associated with neutrophilic pustules in the epidermis. Moreover, the thickening epidermis showed the typical histopathological hallmarks of human psoriatic disease that is acanthosis, parakeratosis, and hyperkeratosis. Therefore, the clinical and histopathological signs developing during the first 7 d of IMQ treatment resembled those present in the early acute phase of human disease in which the first papules are being built. Most histopathological parameters plateaued during the late phase, indicating that the inflammation was fully installed and resembled the stable psoriasis plaques observed in humans (Fig. 1A, 1B). At days 11 and 14 of the late phase, neutrophilic abscesses decreased, whereas epidermal changes stayed pronounced. Time points corresponding to days 5 and 11 are representative of the early and late phases, respectively, and were primarily used in subsequent studies.

### Distinct types of myeloid cells contribute to the early and late phases

We recently established a multicolor phenotyping flow cytometry key enabling to identify LCs, cDC subsets, neutrophils, monocytes, moDCs, and macrophages among the CD45<sup>+</sup>Lin<sup>-</sup> cells of the skin (8, 9). Neutrophils can be identified as Ly-6G<sup>+</sup>CD11b<sup>+</sup> cells

(Supplemental Fig. 1A) (22). MHC II<sup>+</sup> skin cells are composed of LCs, CD11b<sup>-</sup>CD24<sup>+</sup> cDCs (also known as CD103<sup>+</sup> or XCR1<sup>+</sup> DCs), CD11b<sup>+</sup> cDCs (CD24<sup>low</sup>CD11b<sup>+</sup>), and double-negative cDCs (CD11b<sup>-</sup>CD24<sup>-</sup>) (Supplemental Fig. 1B). As shown in Supplemental Fig. 1C, CD11b<sup>+</sup> cDCs can be distinguished from dermal CD11b<sup>+</sup> non-cDCs due to their Ly-6C<sup>-</sup>CD64<sup>-</sup> phenotype. Dermal CD11b<sup>+</sup> non-cDCs can be further resolved on the basis of CCR2 and CD64 expression into CCR2<sup>+</sup>CD64<sup>low</sup> cells that comprise dermal monocytes and Ly-6C<sup>high</sup> and Ly-6C<sup>low</sup> moDCs and CCR2<sup>low</sup>CD64<sup>+</sup> cells that comprise MHC II<sup>low</sup> and MHC II<sup>high</sup> dermal macrophages (Supplemental Fig. 1C). This flow cytometry key kept its discriminatory power when applied to the inflamed skin resulting from IMQ treatment (Supplemental Fig. 1D, 1E).

Analysis of the absolute numbers of each myeloid cell types found in the skin over 14 d of continuous IMQ application showed that neutrophils, monocytes, and Ly-6C<sup>hi</sup> moDCs increased during the early phase and peaked around day 5 (Fig. 2A, 2B). CD11b<sup>-</sup>CD24<sup>+</sup>, CD11b<sup>-</sup>CD24<sup>-</sup>, and CD11b<sup>+</sup> dermal cDCs decreased during the first days of treatment, likely due to their enhanced migration to draining LN. Baseline numbers of dermal cDCs were restored at the end of the treatment period, with CD11b<sup>+</sup> dermal cDCs showing a more rapid rebound (Fig. 2C). Prior to analyzing the dynamics of skin pDCs following IMQ treatment, we noted that PDCA-1 (also known as BST-2 or CD317), a marker commonly used to identify pDCs, was also expressed at intermediate levels on dermal mast cells (data not shown). After excluding dermal mast cells from CD45<sup>+</sup>Lin<sup>-</sup> skin cells on the basis of their CD117 expression, we failed to detect any pDCs, defined on the basis of their expected PDCA-1<sup>+</sup>B220<sup>+</sup>Ly-6C<sup>+</sup>CD11c<sup>low</sup>MHC<sup>-</sup> to <sup>low</sup>CD117<sup>-</sup>CD11b<sup>-</sup> phenotype, in the remaining cells in steady-state skin and during the whole course of IMQ treatment (data not shown). In contrast, using the same phenotyping strategy, pDCs were readily detectable in skin-draining auricular LNs over the whole course of IMQ treatment. These observations are consistent with the fact that pDC ablation had no effect on the magnitude of IMQ-induced psoriatic plaque formation (7, 14).

Dermal macrophages started to increase during the late phase, their numbers plateauing around day 11 (Fig. 2D), whereas LC numbers increased continuously until they peaked at day 11 (Fig. 2D). LC numbers decreased thereafter and reached steady-state levels 20 d after the initiation of continuous IMQ application (data not shown). Therefore, the early and late phases of IMQ-induced psoriatic-like inflammation correlated with the presence of distinct types of myeloid cells, with neutrophils, monocytes, and moDCs dominating the early phase and LCs and macrophages transiently increasing during the late phase (Fig. 2E). This is reminiscent of psoriatic patients, in whom early lesions show an increase in neutrophils, whereas macrophages and cells from the adaptive immune system predominate in stable plaques (23, 24).

### Gene-expression profiling of skin myeloid cell types during the early and late phases of IMQ-induced psoriasis-like inflammation

LCs, CD11b<sup>+</sup> dermal cDCs, monocytes, Ly-6C<sup>high</sup> moDCs, and MHC II<sup>low</sup> and MHC II<sup>high</sup> macrophages were sorted from the skin prior to and after 5 or 11 d of IMQ treatment and subjected to global gene-expression profiling (Supplemental Table I). Two striking observations can be made from hierarchical clustering analysis. First, irrespective of IMQ treatment, LCs clustered together and apart from the other analyzed myeloid cell types (Fig. 3A). Such a feature likely reflects the prenatal origin of LCs, whereas other skin myeloid cell types are generated via adult hematopoiesis (10, 11). Moreover, LCs are the sole type to reside

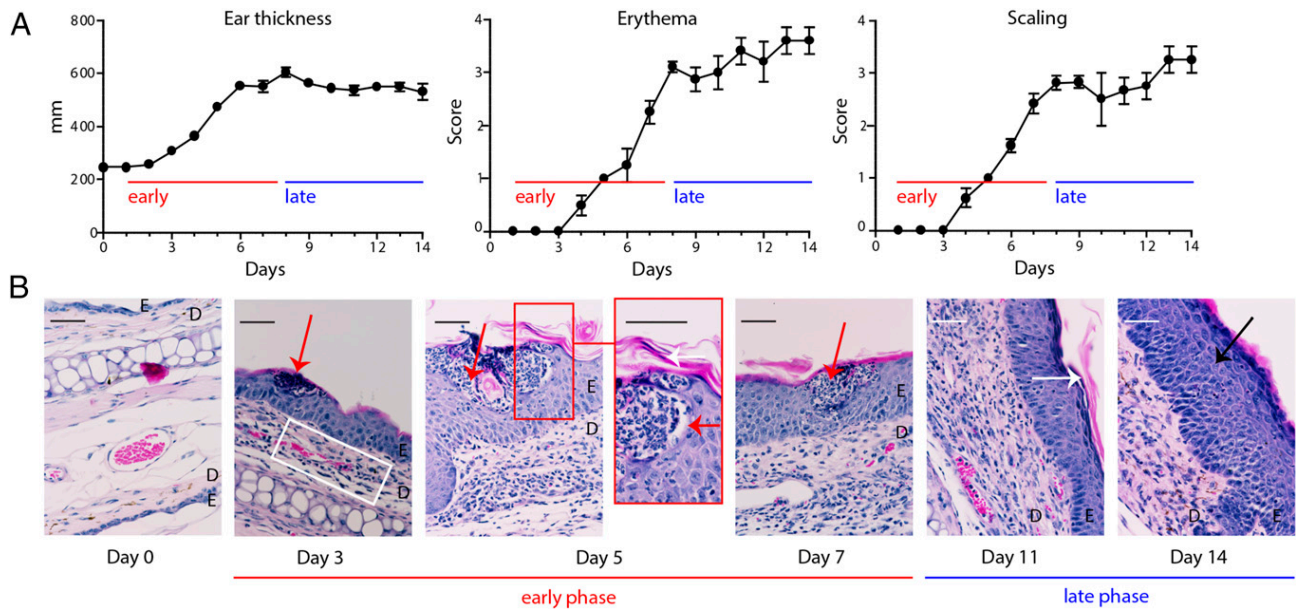


**FIGURE 1.** Long-term application of IMQ recapitulates the early and late phases of human psoriasis. **(A)** IMQ was applied on mouse ear skin for 14 consecutive d, and ear thickness, erythema, and scaling were measured on a daily basis. Erythema and scaling were evaluated according to a score of 1–4 (see *Materials and Methods*). One representative experiment out of three is depicted (mean  $\pm$  SEM). **(B)** Representative H&E staining of histological sections of ears treated for 0, 3, 5, 7, 11, and 14 d with IMQ ( $n \geq 6$  ears/group). The higher magnification provided for day 5 shows that microabscesses consist of an accumulation of granulocytes with lobed and segmented nuclei. A thickening of the stratum corneum (hyperkeratosis) is also noted as compared with day 0. Within the stratum corneum, the flattened nuclei that remain in the corneocytes (white arrow) illustrate the phenomenon of parakeratosis. Histopathological features resembling the human hallmarks of psoriasis are pointed out on representative micrographies. Black arrow, acanthosis; red arrow, epidermal neutrophil microabscess; white arrow, para- and hyperkeratosis; and white square, dense dermal infiltrate and dilatation of blood vessels. Scale bars, 50  $\mu$ m. D, dermis; E, epidermis.

in the epidermis, and this might contribute to their unique pattern of gene expression (25–27). Second, all of the non-LC cell types isolated from IMQ-treated mice clustered together and apart from their counterparts from IMQ-untreated mice. This suggests that a convergent transcriptional reprogramming occurs among all of the non-LC cell types during IMQ treatment. Interestingly, for

most cell types, the samples isolated at days 5 and 11 of IMQ treatment clustered separately, supporting the existence of two distinguishable phases of inflammation development in our long-term IMQ application model.

PCA confirmed and extended the observations deduced from hierarchical clustering. The PC1 axis separated LCs from all of the

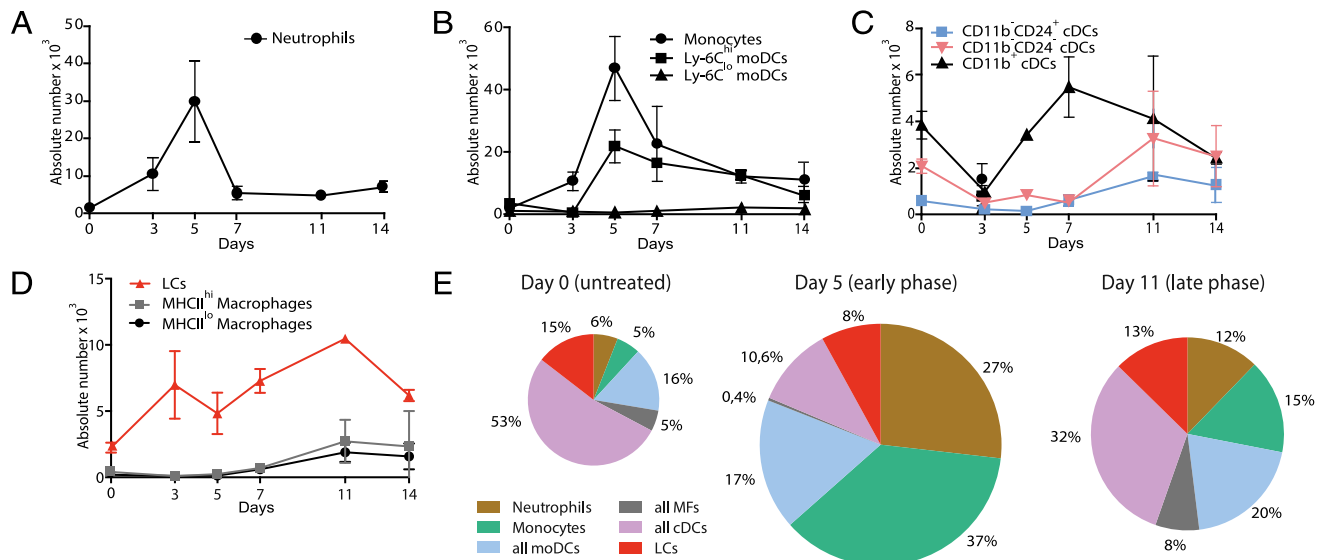


**FIGURE 2.** Distinct skin-infiltrating myeloid cell types characterize the early and late phases of IMQ-induced psoriasis-like inflammation. Single-cell suspensions from mouse ears were analyzed by flow cytometry (see Supplemental Fig. 1), leading to the identification and determination of the absolute numbers of neutrophils **(A)**, dermal monocytes **(B)**, Ly-6C<sup>high</sup> and Ly-6C<sup>low</sup> moDCs **(B)**, CD11b<sup>-</sup>CD24<sup>+</sup>, CD11b<sup>-</sup>CD24<sup>-</sup>, and CD11b<sup>+</sup> dermal cDCs **(C)**, MHC II<sup>low</sup> and MHC II<sup>high</sup> dermal macrophages, and LCs **(D)**. Mean  $\pm$  SEM is depicted. **(E)** Pie chart representation of myeloid cell types found in skin at steady state and after 5 and 11 d of IMQ application. The surface of each chart is proportional to the absolute numbers of myeloid cell types per ear. Data are representative of at least three experiments with  $\geq 3$  animals per condition.

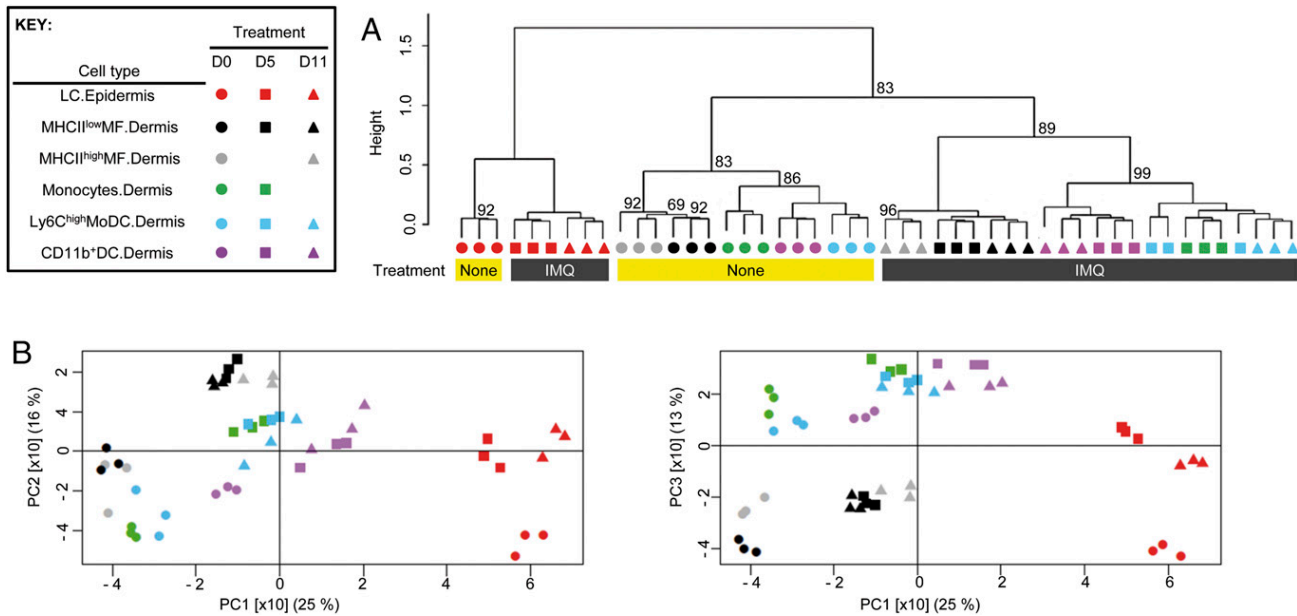


**FIGURE 3.** Gene-expression profiling of skin myeloid cell types during the course of IMQ-induced psoriasis-like inflammation. **(A)** Hierarchical clustering performed on the cell types specified in the key on the top left side prior to (D0) or after 5 (D5) or 11 d (D11) of IMQ treatment. Numbers above nodes indicate their robustness (see *Materials and Methods*). The smaller frequency of Ly-6C<sup>low</sup> moDCs and CD11b<sup>+</sup>CD24<sup>+</sup> and CD11b<sup>+</sup>CD24<sup>-</sup> cDCs found in IMQ-treated skin prevented their analysis, whereas technical issues prevented the analysis of MHC II<sup>high</sup>MF.Dermis.IMQ.D5 and Monocytes.Dermis.IMQ.D11 samples. **(B)** PCA of gene expression by the six cell types prior to and after IMQ treatment (see Key).

other non-LC cell types, irrespective of IMQ treatment (Fig. 3B), a finding consistent with the two primary branches observed in hierarchical clustering. The PC2 axis separated untreated from IMQ-treated cells, showing that IMQ affected all cell types, including LCs, in a convergent manner. A result confirmed by the analysis of the individual expression patterns of genes contributing the most to the PC2 axis (Supplemental Table I). This convergence is illustrated in Supplemental Fig. 2A and 2B for a few selected genes, among which stand out the *S100a8* and *S100a9* genes, among which stand out the *S100a8* and *S100a9* genes, which code for microbicidal and chemotactic alarmins (28). Elevated S100A8 and S100A9 protein levels are a hallmark of human psoriasis, contributing to sterility of the psoriatic plaques and to noxious proinflammatory effects (28, 29). Akin to PC2, the PC3 axis separated untreated from IMQ-treated cells, and, in the case of LCs and CD11b<sup>+</sup> cDCs, it also separated those isolated after 5 and 11 d of IMQ treatment. Indeed, several of the genes contributing the most to the PC3 axis were differentially regulated at day 5 or 11 of IMQ treatment in at least one of the cell types examined (Supplemental Fig. 2C, 2D, Supplemental Table I). For instance, after 5 d of IMQ treatment, LCs selectively and transiently expressed three genes coding for endopeptidase inhibitors (*Stfa211*, *Staf2*, and *Serpib9* in Supplemental Fig. 2E). The protein encoded by *Serpib9* belongs to serpins and may prevent lysis by cytotoxic T cells (30), whereas *Stfa211* and *Staf2* code for stefins A that are intracellular inhibitors of cysteine cathepsins involved in Ag processing (31).

#### *Psoriatic inflammation is associated with increased expression of canonical IFN-I-responsive genes*

IFN-I plays an important role in human psoriasis (4). Consistent with that view, several IFN-stimulated genes (ISGs), such as *Ifitm1*, *Cd274*, and *Plac8*, were expressed at higher levels after 5 d of IMQ treatment in several of the analyzed cell types (Supplemental Fig. 2C). To determine the effect of prolonged IMQ treatment on ISG expression in skin myeloid cells, we performed GeneSet Enrichment Analyses (GSEA) using an ISG gene

set that encompasses all known ISGs (20) and a “KC\_IFN $\alpha$ \_UP” gene set that corresponds to genes reported to be significantly induced by IFN-I in cultured keratinocytes (4). We also used the C2-curated gene set that contains 4722 molecular signatures (18). After 5 d of IMQ treatment, LCs were the sole to be significantly enriched for the ISG gene set, whereas all other analyzed cell types were enriched for the KC\_IFN $\alpha$ \_UP gene set at day 5, and even at day 11 for some of them (Supplemental Fig. 2F). The higher expression of ISGs noted for LCs after 5 d of IMQ treatment turned out to be due to the fact that at steady state, they expressed much lower level of ISGs than the other cell types examined. Accordingly, the rather minor increase in ISG expression that occurred in LCs after 5 d of IMQ treatment translated in substantial fold changes over steady-state conditions and thus biased the GSEA. Therefore, LCs expressed most ISGs at low levels prior to and after IMQ treatment, a feature that likely contributes to maintain epidermal homeostasis. However, after IMQ treatment, LCs and to a lesser extent CD11b<sup>+</sup> dermal cDCs selectively and strongly expressed the *Ifi205*, *Mreg*, and *Fscn1* ISGs (Supplemental Fig. 2G). *Fscn1* expression has been associated with DC maturation (32). In contrast to the situation observed for LCs, continuous IMQ treatment induced a substantial increase in the expression of large numbers of canonical ISGs in all of the non-LC cell types examined (Supplemental Fig. 2G, Supplemental Table I), suggesting that IFN-I play an important role in the long-term IMQ application model.

#### *The unfolding of psoriatic inflammation is associated with enhanced LC proliferation*

The most impressive enrichment observed in GSEA corresponded to gene sets associated with cell proliferation and denoted as “CCNB2” and “Cell cycle” (20) (Supplemental Fig. 2F). LCs and MHC II<sup>low</sup> macrophages found in the skin after 5 and 11 d of IMQ-treatment showed the highest enrichment in these gene sets. Mitosis-associated genes were overexpressed in LCs both after 5 and 11 d of IMQ treatment, whereas their expression peaked

after 5 d of IMQ treatment in MHC II<sup>low</sup> dermal macrophages (Supplemental Fig. 2H, Supplemental Table I).

To corroborate the presence of proliferating LCs in psoriatic lesions, we analyzed whether LCs expressed Ki67, a nuclear protein that characterizes actively cycling cells. Confocal microscopy of skin sections from *LangEGFP* mice that express a GFP under the control of the gene coding for langerin (CD207) allowed the visualization of epidermal LCs on the basis of EGFP expression and epidermal localization (17). Among the EGFP<sup>+</sup> cells present in the skin of *LangEGFP* mice that had been treated with IMQ for 11 d, 22.6 ± 2.4% were Ki67<sup>+</sup>, whereas none of those found in untreated control *LangEGFP* mice were Ki67<sup>+</sup> (Fig. 4A). Quantification by flow cytometry of the increase in Ki67<sup>+</sup> LCs over the course of IMQ application showed a peak at day 9 when ~30% of the LCs were Ki67<sup>+</sup> (Fig. 4B). Congruent with those results, when mice were exposed to BrdU for 4 d prior to the end of IMQ treatment, ~15% of the LCs had incorporated BrdU as compared with <5% in untreated control mice (Fig. 4C). Importantly, analysis of separated epidermal and dermal sheets demonstrated that the increase in the total numbers of LCs was exclusively due to their accumulation in the epidermis (Fig. 4D).

To determine whether the increase in epidermal LCs observed during the course of IMQ treatment resulted from their impaired

migration to skin draining LNs, we combined IMQ treatment with epicutaneous application of TRITC, a fluorescent dye that labels skin DCs and allows to track them during their migration to LN. Analysis of ear-draining LNs after 11 d of IMQ application revealed a strong increase of TRITC<sup>+</sup> cells among CD103<sup>-</sup>CD24<sup>+</sup> migratory cells as compared with control mice (Fig. 4E). Considering that CD103<sup>-</sup>CD24<sup>+</sup> migratory cells comprise both LCs and CD103<sup>-</sup>CD24<sup>+</sup> dermal cDCs, we relied on the fact that LCs are radioresistant to distinguish them from radiosensitive CD103<sup>-</sup>CD24<sup>+</sup> dermal cDCs (12). Accordingly, lethally irradiated B6 (CD45.1 × CD45.2) mice were reconstituted with BM cells isolated from B6 (CD45.1) mice. Analysis of the LN draining the ear of B6 (CD45.1) → B6 (CD45.1 × CD45.2) BM chimeras after 11 d of IMQ treatment showed that the 10-fold increase in the absolute number of CD103<sup>-</sup>CD24<sup>+</sup> migratory cells was fully accounted by radioresistant, host-derived migratory LCs (Fig. 4F). Therefore, the increase in LC numbers observed in the epidermis of IMQ-treated ear did not result from impaired migration of epidermal LCs to the LN. When considered together with a recent study demonstrating that BM-derived cells that infiltrate the inflamed skin during IMQ treatment do not differentiate into epidermal LCs (7), our results suggest that LC accumulation in the epidermis of IMQ-induced psoriatic skin lesions is primarily due

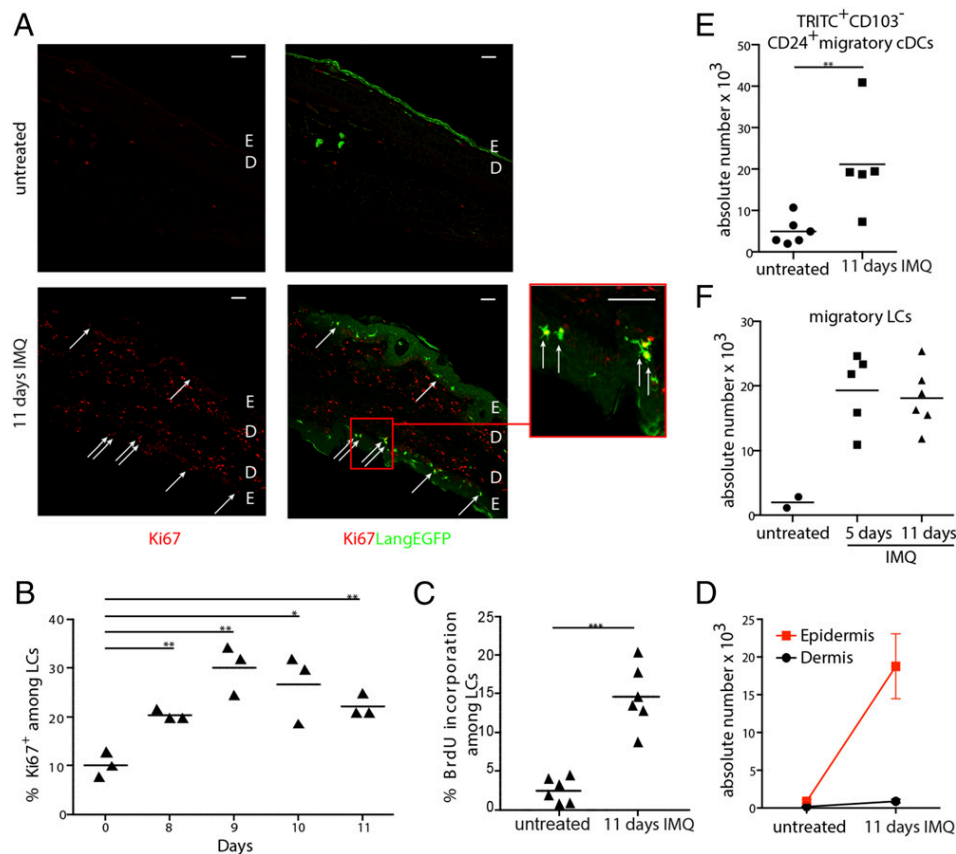


**FIGURE 4.** LCs proliferate during the late phase of psoriatic inflammation. Mice were left untreated, or their ears were treated for the specified period with IMQ. **(A)** Histological sections of ears from *LangEGFP* mice were stained for Ki67 (red) and EGFP (green). Arrows indicate double-positive cells. Representative examples of ≥6 ears per condition are shown. A higher magnification highlighting four Ki67<sup>+</sup> LCs is provided. Scale bars, 80 μm. **(B)** Ears of wild-type mice were left untreated (0) or treated for 8, 9, 10, or 11 d with IMQ, and the percentage of Ki67<sup>+</sup> cells among LCs was assessed by flow cytometry. **(C)** Mice were treated for 11 d with IMQ and received BrdU for the last 4 d of IMQ treatment (11 d IMQ) or solely received BrdU for 4 d (untreated). The percentage of BrdU<sup>+</sup> cells among LCs was determined. **(D)** The epidermis and dermis of the ear skin were separated, and LCs were quantified as in Fig. 2D and Supplemental Fig. 1B. Error bars represent means ± SEM. **(E)** Absolute numbers of TRITC<sup>+</sup> CD103<sup>-</sup>CD24<sup>+</sup> migratory cDCs extracted from skin-draining LNs. **(F)** Absolute numbers of radioresistant migratory LCs extracted from the skin-draining LNs of B6 (CD45.1) → B6 (CD45.1 × CD45.2) BM chimeras. In (B), (C), (E), and (F), each dot corresponds to a mouse, and the mean is indicated. One out of two to three representative experiments is depicted. \**p* < 0.05, \*\**p* < 0.01, \*\*\**p* < 0.005. D, dermis; E, epidermis.

to local proliferation of the LC pool and that those LCs are distinct from the BM-derived, short-lived LCs that develop in the skin following UV irradiation (33).

#### LC depletion led to increased numbers of neutrophils in the late phase of inflammation

The activation status of the LCs and cDCs found in the skin during the long-term IMQ application model was assessed by measuring the levels of expression of CD80, CD40, and MHC II molecules at their surface. Upon IMQ application, LCs showed an upregulation of all of the analyzed activation markers whereas CD11b<sup>-</sup>CD24<sup>+</sup>, CD11b<sup>-</sup>CD24<sup>-</sup>, and CD11b<sup>+</sup> dermal cDCs showed no detectable changes (Supplemental Fig. 3 and data not shown). Considering that upon IMQ treatment, LCs initially increased in number and were the only one to show robust signs of activation, we next analyzed their contribution to the pathology that develops in our biphasic IMQ application model. We used *LangDTREGFP* knockin mice in which it is possible to ablate Langerin-positive DCs following treatment with DT (17). Both LCs and CD11b<sup>-</sup>CD24<sup>+</sup> dermal cDCs express Langerin (34). However, after in vivo DT treatment, LCs and CD11b<sup>-</sup>CD24<sup>+</sup> dermal cDCs repopulate the skin with different kinetics. CD11b<sup>-</sup>CD24<sup>+</sup> cDCs are reconstituted at day 13 after DT administration, whereas LCs are undetectable for up to 30 d after DT administration (34). Therefore, IMQ treatment was started 13 d after the last DT injection, a time point at which LCs were absent, and the adventitious effect of DT treatment noted in some models were no longer significant (9), and pursued for 11 d. A similar IMQ treatment was applied to *LangDTREGFP* mice that received no DT. The lack of LCs had no detectable influence on measured clinical parameters, although there was a trend during the late phase toward stronger inflammation (Fig. 5A). Importantly, flow cytometry analysis of cell suspensions from ear skin revealed that in the absence of LCs, the

late phase of inflammation was characterized by a significantly stronger influx of neutrophils, whereas the other myeloid cell types found in the skin showed no significant differences (Fig. 5B and not shown). We used MMP9, a tertiary granule protein that is formed in mature granulocytes with band-shaped nuclei (35), to determine whether the increase in neutrophil numbers observed in the absence of LCs occurred in the epidermis. Confocal microscopy of MMP9-stained ear skin section of IMQ-treated *LangDTREGFP* mice that lack LCs showed typical neutrophilic epidermal abscesses as compared with IMQ-treated *LangDTREGFP* mice that contain LCs (Fig. 5C), a result supported by H&E staining (Fig. 5D). Therefore, in the absence of LCs, a significant epidermal accumulation of neutrophils occurred during the late phase of the long-term IMQ application model of psoriasis-like inflammation.

#### Discussion

Psoriasis occurs in various clinical subtypes and encompasses two phases. In humans, the early lesions of plaque-type psoriasis and pustular types of psoriasis are dominated by neutrophil infiltrates and later on evolve into fully established chronic plaques that are associated with Th1 and -17 adaptive immunity (24). Preclinical studies on psoriasis have been hampered by the lack of animal models mimicking the biphasic course of the human disease. In the current study, we describe a mouse model that requires daily application of IMQ on the mouse ear skin for 14 d and recapitulates both the early and late phases of the human disease and their associated clinical and histopathological hallmarks. It resembles other models of chronic diseases such as chronic hypersensitivity reactions, in which a continuous stimulus is required to maintain the chronic inflammation. In the case of psoriasis, the exact nature of this causative stimulus remains unknown. In hu-

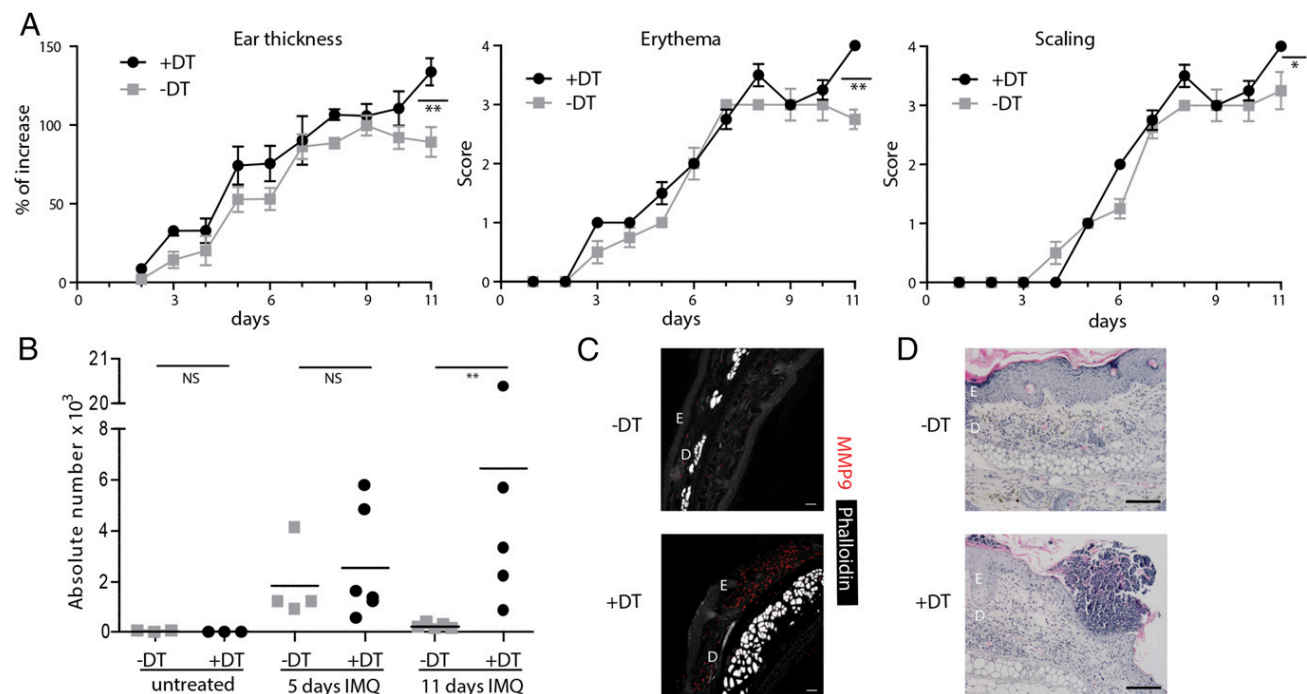


**FIGURE 5.** The lack of LCs during the whole course of the inflammation results in increased numbers of neutrophils during the late phase of psoriatic inflammation. IMQ application for 0, 5, or 11 d on ears of *LangDTREGFP* mice for which LCs have been depleted via injection of DT (+DT) or left untouched (-DT). (A) Ear thickness, erythema, and scaling were measured daily. Increase in ear thickness was calculated as percent of thickness at day 0. (B) Absolute numbers of neutrophils in the ear skin of *LangDTREGFP* mice. (A and B) One representative experiment is depicted out of three (mean ± SEM). (C) Ear sections were stained for MMP9 (red) and phalloidin (white). Scale bars, 50 μm. (D) Representative H&E staining of ear section of *LangDTREGFP* mice. Scale bars, 100 μm. (C and D) ≥6 ears were analyzed per conditions. \**p* < 0.05, \*\**p* < 0.01.

man, IMQ-induced psoriasis-like inflammation withdrawal of the trigger leads to resolution of the skin lesions (36), an observation consistent with our mouse model, which also requires continuous application of IMQ.

Reminiscent of psoriatic patients, monocytes, neutrophils, and moDCs dominate the early phase of our biphasic model. During the late phase, the numbers of neutrophils and monocytes rapidly decrease, whereas dermal macrophages together with LCs initially increase and subsequently decrease. Such transient epidermal LC expansion resulted in an increase rate of LC migration to the skin-draining LNs. Consistent with our observation, a recent study using a mouse model of psoriasis inflammation based on tamoxifen-induced deletion of the Jun and JunB transcription factors (DKO\* mice) showed an increase in LC numbers at day 7 followed by a decrease at day 14 (7). Such transient LC expansion that occurred within the thickened epidermis is due to local proliferation of LCs, a mechanism that has been described for the self-renewal of epidermal LC pool in steady-state conditions and during atopic dermatitis, respectively (10). In support of our observation, transcriptomic analysis indicated that the LCs found in the skin after 5 and 11 d of IMQ treatment highly expressed genes linked to cell cycling. Interestingly, the presence of proliferating LCs had been also reported in human psoriasis (37).

The function played by LCs in different mouse models of psoriasis-like inflammation has been controversial (14, 38, 39). A single study, based on DKO\* mice, analyzed the late phase of psoriasis-like inflammation and suggested that LCs exert a negative immunoregulatory role via IL-10 and programmed cell death ligand-1 (7). Likewise, our results that are based on long-term IMQ application suggest a negative immunoregulatory role for the proliferating and activated LCs found in the epidermis of established psoriatic lesions. We showed that genetic depletion of the LCs during the whole course of the inflammation resulted in a late phase associated with increased neutrophil infiltration and extended pustular lesions. In conclusion, by developing a mouse model with a biphasic course of IMQ-induced psoriasis-like inflammation and combining it to a fine-grained analysis of the dynamics of skin myeloid cells, we were able to support the presumptive anti-inflammatory role of LCs during psoriasis-like inflammation. Moreover, pDCs were absent from the skin during the whole course of the psoriasis-like inflammation, an observation consistent with the fact that their ablation had no effect on the magnitude of IMQ-induced psoriatic plaque formation (7, 14).

## Acknowledgments

We thank F. Baudimont and L. Chasson for assistance with histology and K. Molawi for discussion.

## Disclosures

The authors have no financial conflicts of interest.

## References

- Nestle, F. O., D. H. Kaplan, and J. Barker. 2009. Psoriasis. *N. Engl. J. Med.* 361: 496–509.
- Lande, R., E. Botti, C. Jandus, D. Dojcinovic, G. Fanelli, C. Conrad, G. Chamilos, L. Feldmeyer, B. Marinari, S. Chon, et al. 2014. The antimicrobial peptide LL37 is a T-cell autoantigen in psoriasis. *Nat. Commun.* 5: 5621.
- Di Cesare, A., P. Di Meglio, and F. O. Nestle. 2009. The IL-23/Th17 axis in the immunopathogenesis of psoriasis. *J. Invest. Dermatol.* 129: 1339–1350.
- Lowes, M. A., M. Suárez-Fariñas, and J. G. Krueger. 2014. Immunology of psoriasis. *Annu. Rev. Immunol.* 32: 227–255.
- Nestle, F. O., C. Conrad, A. Tun-Kyi, B. Homey, M. Gombert, O. Boyman, G. Burg, Y. J. Liu, and M. Gilliet. 2005. Plasmacytoid dendritic cells initiate psoriasis through interferon-alpha production. *J. Exp. Med.* 202: 135–143.
- Ganguly, D., G. Chamilos, R. Lande, J. Gregorio, S. Meller, V. Facchinetti, B. Homey, F. J. Barrat, T. Zal, and M. Gilliet. 2009. Self-RNA-antimicrobial peptide complexes activate human dendritic cells through TLR7 and TLR8. *J. Exp. Med.* 206: 1983–1994.
- Glitzner, E., A. Korosec, P. M. Brunner, B. Drobits, N. Amberg, H. B. Schonhauer, T. Kopp, E. F. Wagner, G. Stingl, M. Holcman, and M. Sibilia. 2014. Specific roles for dendritic cell subsets during initiation and progression of psoriasis. *EMBO Mol. Med.* 6: 1312–1327.
- Tamoutounour, S., M. Williams, F. Montanana Sanchis, H. Liu, D. Terhorst, C. Malosse, E. Pollet, L. Ardouin, H. Luche, C. Sanchez, et al. 2013. Origins and functional specialization of macrophages and of conventional and monocyte-derived dendritic cells in mouse skin. *Immunity* 39: 925–938.
- Malissen, B., S. Tamoutounour, and S. Henri. 2014. The origins and functions of dendritic cells and macrophages in the skin. *Nat. Rev. Immunol.* 14: 417–428.
- Chorro, L., A. Sarde, M. Li, K. J. Woollard, P. Chambon, B. Malissen, A. Kissenpfennig, J. B. Barbaroux, R. Groves, and F. Geissmann. 2009. Langerhans cell (LC) proliferation mediates neonatal development, homeostasis, and inflammation-associated expansion of the epidermal LC network. *J. Exp. Med.* 206: 3089–3100.
- Hoeffel, G., Y. Wang, M. Greter, P. See, P. Teo, B. Malleret, M. Leboeuf, D. Low, G. Oller, F. Almeida, et al. 2012. Adult Langerhans cells derive predominantly from embryonic fetal liver monocytes with a minor contribution of yolk sac-derived macrophages. *J. Exp. Med.* 209: 1167–1181.
- Henri, S., L. F. Poulin, S. Tamoutounour, L. Ardouin, M. Williams, B. de Bovis, E. Devillard, C. Viret, H. Azukizawa, A. Kissenpfennig, and B. Malissen. 2010. CD207+ CD103+ dermal dendritic cells cross-present keratinocyte-derived antigens irrespective of the presence of Langerhans cells. *J. Exp. Med.* 207: 189–206.
- Riol-Blanco, L., J. Ordovas-Montanes, M. Perro, E. Naval, A. Thiriou, D. Alvarez, S. Paust, J. N. Wood, and U. H. von Andrian. 2014. Nociceptive sensory neurons drive interleukin-23-mediated psoriasiform skin inflammation. *Nature* 510: 157–161.
- Wohn, C., J. L. Ober-Biöbaum, S. Haak, S. Pantelyushin, C. Cheong, S. P. Zahner, S. Onderwater, M. Kant, H. Weighardt, B. Holzmann, et al. 2013. Langerin(neg) conventional dendritic cells produce IL-23 to drive psoriatic plaque formation in mice. *Proc. Natl. Acad. Sci. USA* 110: 10723–10728.
- Flutter, B., and F. O. Nestle. 2013. TLRs to cytokines: mechanistic insights from the imiquimod mouse model of psoriasis. *Eur. J. Immunol.* 43: 3138–3146.
- Swindell, W. R., A. Johnston, S. Carbajal, G. Han, C. Wohn, J. Lu, X. King, R. P. Nair, J. J. Voorhees, J. T. Elder, et al. 2011. Genome-wide expression profiling of five mouse models identifies similarities and differences with human psoriasis. *PLoS One* 6: e18266.
- Kissenpfennig, A., S. Henri, B. Dubois, C. Laplace-Builhé, P. Perrin, N. Romani, C. H. Tripp, P. Douillard, L. Leserman, D. Kaiserlian, et al. 2005. Dynamics and function of Langerhans cells in vivo: dermal dendritic cells colonize lymph node areas distinct from slower migrating Langerhans cells. *Immunity* 22: 643–654.
- Subramanian, A., H. Kuehn, J. Gould, P. Tamayo, and J. P. Mesirov. 2007. GSEA-P: a desktop application for Gene Set Enrichment Analysis. *Bioinformatics* 23: 3251–3253.
- Baranek, T., T. P. Manh, Y. Alexandre, M. A. Maqbool, J. Z. Cabeza, E. Tomasello, K. Crozat, G. Bessou, N. Zucchini, S. H. Robbins, et al. 2012. Differential responses of immune cells to type I interferon contribute to host resistance to viral infection. *Cell Host Microbe* 12: 571–584.
- Balan, S., V. Ollion, N. Colletti, R. Chelbi, F. Montanana-Sanchis, H. Liu, T. P. Vu Manh, C. Sanchez, J. Savoret, I. Perrot, et al. 2014. Human XCR1+ dendritic cells derived in vitro from CD34+ progenitors closely resemble blood dendritic cells, including their adjuvant responsiveness, contrary to monocyte-derived dendritic cells. *J. Immunol.* 193: 1622–1635.
- van der Fits, L., S. Mourits, J. S. Voerman, M. Kant, L. Boon, J. D. Laman, F. Cornelissen, A. M. Mus, E. Florencia, E. P. Prens, and E. Lubberts. 2009. Imiquimod-induced psoriasis-like skin inflammation in mice is mediated via the IL-23/IL-17 axis. *J. Immunol.* 182: 5836–5845.
- Gregorio, J., S. Meller, C. Conrad, A. Di Nardo, B. Homey, A. Lauerma, N. Arai, R. L. Gallo, J. Digiovanni, and M. Gilliet. 2010. Plasmacytoid dendritic cells sense skin injury and promote wound healing through type I interferons. *J. Exp. Med.* 207: 2921–2930.
- Murphy, M., P. Kerr, and J. M. Grant-Kels. 2007. The histopathologic spectrum of psoriasis. *Clin. Dermatol.* 25: 524–528.
- Christophers, E., G. Metzler, and M. Röcken. 2014. Bimodal immune activation in psoriasis. *Br. J. Dermatol.* 170: 59–65.
- Elpek, K. G., A. Bellemare-Pelletier, D. Malhotra, E. D. Reynoso, V. Lukacs-Kornek, R. H. DeKruyff, and S. J. Turley. 2011. Lymphoid organ-resident dendritic cells exhibit unique transcriptional fingerprints based on subset and site. *PLoS One* 6: e23921.
- Gosselin, D., V. M. Link, C. E. Romanoski, G. J. Fonseca, D. Z. Eichenfield, N. J. Spann, J. D. Stender, H. B. Chun, H. Garner, F. Geissmann, and C. K. Glass. 2014. Environment drives selection and function of enhancers controlling tissue-specific macrophage identities. *Cell* 159: 1327–1340.
- Epelman, S., K. J. Lavine, A. E. Beaudin, D. K. Sojka, J. A. Carrero, B. Calderon, T. Brijia, E. L. Gautier, S. Ivanov, A. T. Satpathy, et al. 2014. Embryonic and adult-derived resident cardiac macrophages are maintained through distinct mechanisms at steady state and during inflammation. *Immunity* 40: 91–104.
- Gebhardt, C., J. Németh, P. Angel, and J. Hess. 2006. S100A8 and S100A9 in inflammation and cancer. *Biochem. Pharmacol.* 72: 1622–1631.
- Kerkhoff, C., A. Voss, T. E. Scholzen, M. M. Averill, K. S. Zänker, and K. E. Bornfeldt. 2012. Novel insights into the role of S100A8/A9 in skin biology. *Exp. Dermatol.* 21: 822–826.

30. Andrew, K. A., H. M. Simkins, S. Witzel, R. Perret, J. Hudson, I. F. Hermans, D. S. Ritchie, J. Yang, and F. Ronchese. 2008. Dendritic cells treated with lipopolysaccharide up-regulate serine protease inhibitor 6 and remain sensitive to killing by cytotoxic T lymphocytes in vivo. *J. Immunol.* 181: 8356–8362.
31. Chapman, H. A. 2006. Endosomal proteases in antigen presentation. *Curr. Opin. Immunol.* 18: 78–84.
32. Manh, T. P., Y. Alexandre, T. Baranek, K. Crozat, and M. Dalod. 2013. Plasmacytoid, conventional, and monocyte-derived dendritic cells undergo a profound and convergent genetic reprogramming during their maturation. *Eur. J. Immunol.* 43: 1706–1715.
33. Seré, K., J. H. Baek, J. Ober-Blöbaum, G. Müller-Newen, F. Tacke, Y. Yokota, M. Zenke, and T. Hieronymus. 2012. Two distinct types of Langerhans cells populate the skin during steady state and inflammation. *Immunity* 37: 905–916.
34. Poulin, L. F., S. Henri, B. de Bovis, E. Devilard, A. Kissenpfennig, and B. Malissen. 2007. The dermis contains langerin+ dendritic cells that develop and function independently of epidermal Langerhans cells. *J. Exp. Med.* 204: 3119–3131.
35. Fauschou, M., and N. Borregaard. 2003. Neutrophil granules and secretory vesicles in inflammation. *Microbes Infect.* 5: 1317–1327.
36. Fanti, P. A., E. Dika, S. Vaccari, C. Miscial, and C. Varotti. 2006. Generalized psoriasis induced by topical treatment of actinic keratosis with imiquimod. *Int. J. Dermatol.* 45: 1464–1465.
37. Bata-Csorgo, Z., C. Hammerberg, J. J. Voorhees, and K. D. Cooper. 1993. Flow cytometric identification of proliferative subpopulations within normal human epidermis and the localization of the primary hyperproliferative population in psoriasis. *J. Exp. Med.* 178: 1271–1281.
38. Greter, M., I. Lelios, P. Pelczar, G. Hoeffel, J. Price, M. Leboeuf, T. M. Kündig, K. Frei, F. Ginhoux, M. Merad, and B. Becher. 2012. Stroma-derived interleukin-34 controls the development and maintenance of langerhans cells and the maintenance of microglia. *Immunity* 37: 1050–1060.
39. Yoshiki, R., K. Kabashima, T. Honda, S. Nakamizo, Y. Sawada, K. Sugita, H. Yoshioka, S. Ohmori, B. Malissen, Y. Tokura, and M. Nakamura. 2014. IL-23 from Langerhans cells is required for the development of imiquimod-induced psoriasis-like dermatitis by induction of IL-17A-producing  $\gamma\delta$  T cells. *J. Invest. Dermatol.* 134: 1912–1921.